

$R(J/\psi)$ and $B_c^- \rightarrow J/\psi \ell^- \bar{\nu}_\ell$ Lepton Flavor Universality Violating Observables from Lattice QCD

Judd Harrison^{1,*} Christine T. H. Davies^{1,†} and Andrew Lytle^{1,‡}

(HPQCD Collaboration)[‡]

¹SUPA, School of Physics and Astronomy, University of Glasgow, Glasgow, G12 8QQ, United Kingdom

²INFN, Sezione di Roma Tor Vergata, Via della Ricerca Scientifica 1, 00133 Roma RM, Italy



(Received 22 July 2020; accepted 15 October 2020; published 24 November 2020)

We use our lattice QCD computation of the $B_c \rightarrow J/\psi$ form factors to determine the differential decay rate for the semitauonic decay channel and construct the ratio of branching fractions $R(J/\psi) = \mathcal{B}(B_c^- \rightarrow J/\psi \tau^- \bar{\nu}_\tau)/\mathcal{B}(B_c^- \rightarrow J/\psi \mu^- \bar{\nu}_\mu)$. We find $R(J/\psi) = 0.2582(38)$ and give an error budget. We also extend the relevant angular observables, which were recently suggested for the study of lepton flavor universality violating effects in $B \rightarrow D^* \ell \nu$, to $B_c \rightarrow J/\psi \ell \nu$ and make predictions for their values under different new physics scenarios.

DOI: 10.1103/PhysRevLett.125.222003

Introduction.— B -meson exclusive semileptonic decay processes are powerful tests of the Standard model (SM) in cases where both experimental and theoretical uncertainties can be brought under control. They allow for the determination of elements of the Cabibbo-Kobayashi-Maskawa matrix and tests of its unitarity but are also more detailed probes for new physics scenarios. An exciting possibility is that of nonuniversality of the couplings of charged leptons in electroweak interactions, hinted at in measurements of the ratio, \mathcal{R} , of the branching fraction to τ in the final state to that of μ/e for $B \rightarrow D^{(*)}$ [1–10],

$$\mathcal{R}(D^{(*)}) = \frac{\mathcal{B}(B \rightarrow D^{(*)} \tau \bar{\nu}_\tau)}{\mathcal{B}(B \rightarrow D^{(*)} \mu \bar{\nu}_\mu)}. \quad (1)$$

The combination of experimental results for $\mathcal{R}(D)$ and $\mathcal{R}(D^*)$ is in tension with the SM at 3.1σ [11,12]. This includes a recent result from Belle [10] using semileptonic tagging, which by itself agrees with the SM within 1.6σ . Most of the pull comes from $\mathcal{R}(D^*)$ for which the SM results being used [13–15] rely on arguments from sum rules and heavy quark effective theory because lattice QCD results, which provide the best *ab initio* determination of the form factors, are as yet only available for the A_1 form factor at a zero recoil [16,17]. Extending the lattice QCD

calculation to cover more of the q^2 range is underway [18,19].

This motivates a study of \mathcal{R} for other $b \rightarrow c$ semileptonic decay modes, and LHCb recently gave the first results for $\mathcal{R}(J/\psi)$ from a $B_c \rightarrow J/\psi$ decay [20]. They found $R(J/\psi) = 0.71 \pm 0.17_{\text{stat}} \pm 0.18_{\text{sys}}$ and compared it to SM results from a variety of model calculations. Since it is difficult to quantify uncertainties from individual models, the spread of results between models must be taken as a measure of this. LHCb quote a range of SM values from 0.25 to 0.28 from [21–24], giving a 10% spread. Since this is the same level as the discrepancy seen in $\mathcal{R}(D^*)$ currently, it is unlikely that this accuracy would be good enough to distinguish experiment (given improved uncertainties there) and the SM. More recent results see a similar spread [25–27]. In addition, the dominant systematic error for the experiment comes from the uncertainty in input form factors for $B_c \rightarrow J/\psi$ from these models.

In [28], we have given results for the $B_c \rightarrow J/\psi$ form factors from lattice QCD for the first time. We work on gluon field configurations that include u, d, s , and c quarks in the sea and use a discretization of the Dirac equation, which was developed by the HPQCD Collaboration to have particularly small discretization errors [29]. This makes it suitable for handling heavy b and c quarks where discretization errors are relatively large. It also enables us to use a relativistic formalism in which the quark currents that couple to the W boson can be normalized in a fully nonperturbative way. We use HPQCD's "heavy-HISQ" technique, which has been successful in determining the decay constants of heavy-light mesons [30–33] and is now being applied to B semileptonic form factors [34,35], where

Published by the American Physical Society under the terms of the Creative Commons Attribution 4.0 International license. Further distribution of this work must maintain attribution to the author(s) and the published article's title, journal citation, and DOI. Funded by SCOAP³.

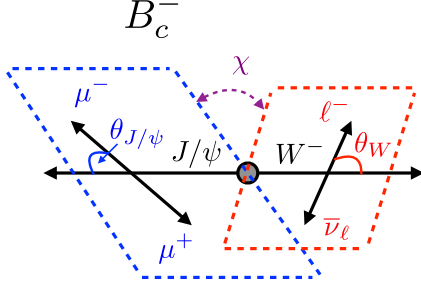


FIG. 1. Conventions for the angular variables entering the differential decay rate.

it enables the full q^2 range of the decay to be covered. Further details can be found in [28], where we give the form factors and derive the total rate and branching fraction for the decay with $\mu\bar{\nu}_\mu$ in the final state. Here, we focus on the $\tau\bar{\nu}_\tau$ mode and determine $\mathcal{R}(J/\psi)$ in the SM with quantified uncertainties. We also give values for asymmetries, which show sensitivity to new physics.

Theoretical background.—We give below the full differential rate [36] for $B_c^- \rightarrow J/\psi \ell^- \bar{\nu}$, where ℓ is a lepton with mass m_ℓ , with respect to squared four-momentum transfer, q^2 , and angles defined in Fig. 1. We assume that the J/ψ is identified through its (purely electromagnetic) decay to $\mu^+\mu^-$, defining the angle $\theta_{J/\psi}$, and we sum over the $\mu^+\mu^-$ helicities,

$$\frac{d^4\Gamma(B_c^- \rightarrow J/\psi(\rightarrow \mu^+\mu^-)\ell^-\bar{\nu})}{d\cos(\theta_{J/\psi})d\cos(\theta_W)d\chi dq^2} = \mathcal{B}(J/\psi \rightarrow \mu^+\mu^-)\mathcal{N}\sum_i k_i(\theta_W, \theta_{J/\psi}, \chi)\mathcal{H}_i(q^2), \quad (2)$$

where

$$\mathcal{N} = \frac{G_F^2}{(4\pi)^4} |\eta_{EW}|^2 |V_{cb}|^2 \frac{3(q^2 - m_\ell^2)^2 |\vec{p}'|}{8M_{B_c}^2 q^2}. \quad (3)$$

Here, $|\vec{p}'|$ is the magnitude of the J/ψ spatial momentum in the B_c rest frame, and η_{EW} is the same structure-independent electroweak correction as in [28], 1.0062(16) [37]. The k_i and \mathcal{H}_i are given in Table I. We include in the expressions terms with factors of m_ℓ^2/q^2 that were dropped in [28]. These are significant for the case when $\ell = \tau$ and include the helicity amplitude H_t which does not otherwise appear. Integrating over angles, the differential rate in q^2 is then given by

$$\frac{d\Gamma}{dq^2} = \mathcal{N} \times \frac{64\pi}{9} \left[(H_-^2 + H_0^2 + H_+^2) + \frac{m_\ell^2}{2q^2} (H_-^2 + H_0^2 + H_+^2 + 3H_t^2) \right]. \quad (4)$$

TABLE I. The helicity amplitude combinations and coefficients for them that appear in the differential rate, Eq. (2).

i	\mathcal{H}_i	$k_i(\theta_W, \theta_{J/\psi}, \chi)$
1	$ H_+(q^2) ^2$	$\frac{1}{2}(1-\cos(\theta_W))^2(1+\cos^2(\theta_{J/\psi}))$
2	$ H_-(q^2) ^2$	$\frac{1}{2}(1+\cos(\theta_W))^2(1+\cos^2(\theta_{J/\psi}))$
3	$ H_0 ^2$	$2\sin^2(\theta_W)\sin^2(\theta_{J/\psi})$
4	$\text{Re}(H_+H_0^*)$	$\sin(\theta_W)\sin(2\theta_{J/\psi})\cos(\chi)(1-\cos(\theta_W))$
5	$\text{Re}(H_-H_0^*)$	$-\sin(\theta_W)\sin(2\theta_{J/\psi})\cos(\chi)(1+\cos(\theta_W))$
6	$\text{Re}(H_+H_-^*)$	$\sin^2(\theta_W)\sin^2(\theta_{J/\psi})\cos(2\chi)$
7	$m_\ell^2/q^2 H_+(q^2) ^2$	$\frac{1}{2}(1-\cos^2(\theta_W))(1+\cos^2(\theta_{J/\psi}))$
8	$m_\ell^2/q^2 H_-(q^2) ^2$	$\frac{1}{2}(1-\cos^2(\theta_W))(1+\cos^2(\theta_{J/\psi}))$
9	$m_\ell^2/q^2 H_0 ^2$	$2\cos^2(\theta_W)\sin^2(\theta_{J/\psi})$
10	$m_\ell^2/q^2 H_t(q^2) ^2$	$2\sin^2(\theta_{J/\psi})$
11	$(m_\ell^2/q^2)\text{Re}(H_+H_0^*)$	$\sin(\theta_W)\sin(2\theta_{J/\psi})\cos(\chi)\cos(\theta_W)$
12	$(m_\ell^2/q^2)\text{Re}(H_-H_0^*)$	$\sin(\theta_W)\sin(2\theta_{J/\psi})\cos(\chi)\cos(\theta_W)$
13	$(m_\ell^2/q^2)\text{Re}(H_+H_-^*)$	$-\sin^2(\theta_W)\sin^2(\theta_{J/\psi})\cos(2\chi)$
14	$(m_\ell^2/q^2)\text{Re}(H_tH_0^*)$	$-4\sin^2(\theta_{J/\psi})\cos(\theta_W)$
15	$(m_\ell^2/q^2)\text{Re}(H_+H_t^*)$	$-\sin(\theta_W)\sin(2\theta_{J/\psi})\cos(\chi)$
16	$(m_\ell^2/q^2)\text{Re}(H_-H_t^*)$	$-\sin(\theta_W)\sin(2\theta_{J/\psi})\cos(\chi)$

The helicity amplitudes are defined in terms of standard Lorentz-invariant form factors [38] as

$$H_\pm(q^2) = (M_{B_c} + M_{J/\psi})A_1(q^2) \mp \frac{2M_{B_c}|\vec{p}'|}{M_{B_c} + M_{J/\psi}} V(q^2),$$

$$H_0(q^2) = \frac{1}{2M_{J/\psi}\sqrt{q^2}} \left(-4 \frac{M_{B_c}^2|\vec{p}'|^2}{M_{B_c} + M_{J/\psi}} A_2(q^2) + (M_{B_c} + M_{J/\psi})(M_{B_c}^2 - M_{J/\psi}^2 - q^2)A_1(q^2) \right),$$

$$H_t(q^2) = \frac{2M_{B_c}|\vec{p}'|}{\sqrt{q^2}} A_0(q^2). \quad (5)$$

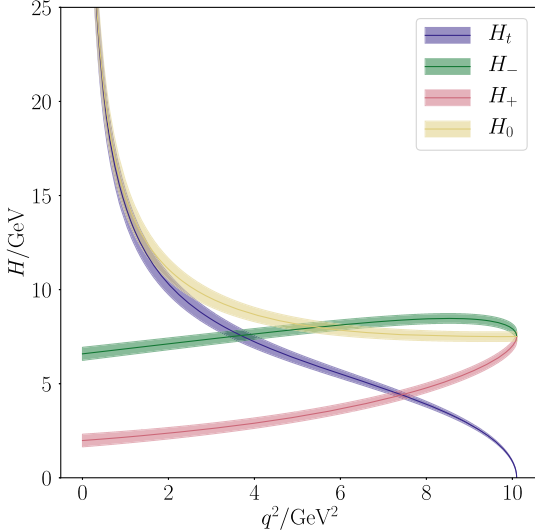
Γ and $R(J/\psi)$.—The form factors were computed across the full physical q^2 range in [28] using lattice QCD. They are given in terms of a polynomial in z , with coefficients a_n^F , and a pole term corresponding to B_c states with the quantum numbers of each current,

$$F(q^2) = \frac{1}{P(q^2)} \sum_{n=0}^3 a_n^F z(t_+, t_-, q^2)^n, \quad (6)$$

for $F = A_0, A_1, A_2, V$, and where

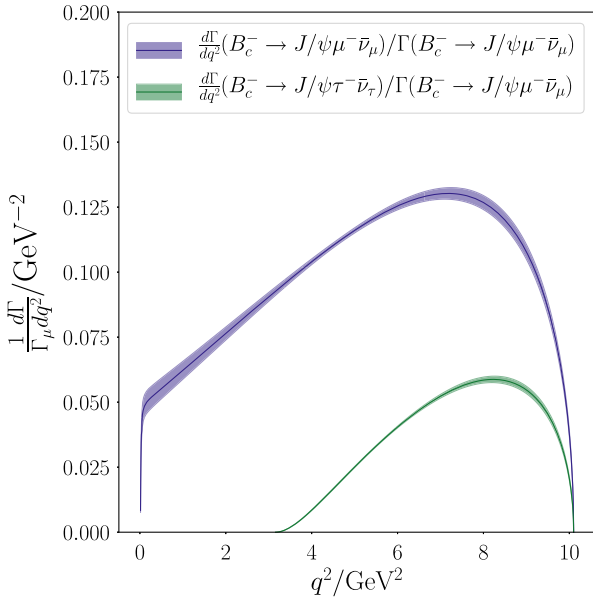
$$z(t_+, t_-, q^2) = \frac{\sqrt{t_+ - q^2} - \sqrt{t_+ - t_-}}{\sqrt{t_+ - q^2} + \sqrt{t_+ - t_-}}. \quad (7)$$

t_- is the maximum value of q^2 , $t_- = (M_{B_c} - M_{J/\psi})^2$, t_+ is the pair production threshold, $t_+ = (M_B + M_{D^*})^2$, and

FIG. 2. Helicity amplitudes [Eq. (5)] plotted as a function of q^2 .

$P(q^2) = \prod_{M_{\text{pole}}} z(t_+, M_{\text{pole}}, q^2)$. The meson and subthreshold resonance masses, M_{pole} , that need to be used in reconstructing the form factors are given in [28]. We assemble the helicity amplitudes using Eq. (5); these are plotted as a function of q^2 in Fig. 2 (Fig. 10 of [28]). Differential and total decay rates are then calculated. Where an integration over q^2 is necessary, we use a simple trapezoidal interpolation in order to ensure covariances are carried through correctly, taking sufficiently many points that the results are insensitive to the addition of any further points.

The differential rate $d\Gamma/dq^2$ is plotted in Fig. 3, comparing SM rates for $\ell = \mu$ and $\ell = \tau$. We also compute the total

FIG. 3. $d\Gamma/dq^2$ in the SM for the $\ell = \mu$ and $\ell = \tau$ cases, normalized to the total rate for $\ell = \mu$, Γ_μ .

decay rates, and from these, $R(J/\psi) = \mathcal{B}(B_c^- \rightarrow J/\psi\tau^-\bar{\nu}_\tau)/\mathcal{B}(B_c^- \rightarrow J/\psi\mu^-\bar{\nu}_\mu)$. We find

$$\begin{aligned} \Gamma(B_c^- \rightarrow J/\psi\mu^-\bar{\nu}_\mu)/|\eta_{\text{EW}} V_{cb}|^2 &= 1.73(12) \times 10^{13} \text{ s}^{-1} \\ &= 11.36(81) \times 10^{-12} \text{ GeV} \\ \Gamma(B_c^- \rightarrow J/\psi\tau^-\bar{\nu}_\tau)/|\eta_{\text{EW}} V_{cb}|^2 &= 4.45(30) \times 10^{12} \text{ s}^{-1} \\ &= 2.93(19) \times 10^{-12} \text{ GeV}, \end{aligned} \quad (8)$$

and their ratio,

$$R(J/\psi) = 0.2582(38). \quad (9)$$

The error budget for these results is given in Table II. The largest contributions for both $\Gamma(\ell = \tau)$ and $\Gamma(\ell = \mu)$ are the discretization effects from the heavy quark mass, the statistical uncertainty in the lattice data, and the quark mass mistunings effects. These errors and their potential improvement are discussed in [28]. There is significant cancellation of these correlated errors in \mathcal{R} , resulting in a factor of ≈ 5 reduction in uncertainty compared to Γ , and leaving the dominant error that from lattice statistics. The value for $R(J/\psi)$ is very close to that expected in the SM for $R(D^*)$ [12]. $R(J/\psi)$ is given here as the ratio of the rates to τ and μ ; we showed in [28] that the decay rates to μ and e differ by 0.4%.

R^{NP}(J/ψ), angular observables and tests of lepton flavor universality.—The effects of new physics (NP) may be considered through the inclusion of complex-valued NP couplings, g_i , $i \in S, P, V, A, T, T5$, in the effective Hamiltonian describing $b \rightarrow c\ell\nu$ decays [39]. Reference [40] takes new physics to appear in the $\ell = \tau$ channel only and fits the g_i individually against the experimental average values of $R(D)$ and $R(D^*)$. Angular observables sensitive to the different NP scenarios are then constructed. Here, we use the values of g for

TABLE II. Error budget for Γ for the cases $\ell = \tau$ and $\ell = \mu$ and their ratio, $\mathcal{R}(J/\psi)$. Errors are given as a percentage of the final answer. See [28] for more details.

Source	$\Gamma/ \eta_{\text{EW}} V_{cb} ^2$		
	$\ell = \mu$	$\ell = \tau$	$R(J/\psi)$
m_h dependence	2.4	2.2	0.6
Continuum limit	3.8	3.6	0.8
Sea-quark mass effects	3.6	3.4	0.3
Lattice spacing determination	1.4	1.3	0.1
Statistics	3.6	3.2	1.1
Other	1.6	1.5	0.0
Total (%)	7.2	6.6	1.5

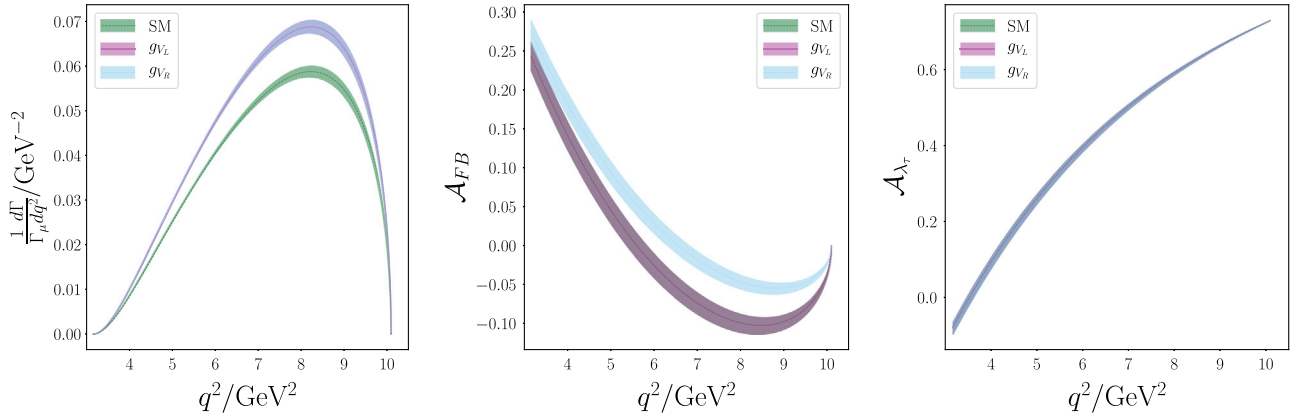


FIG. 4. $d\Gamma/dq^2$, A_{FB} , and A_{λ_τ} for $B_c^- \rightarrow J/\psi \tau^- \bar{\nu}_\tau$ in the SM and for the values of g_{V_R} and g_{V_L} given in Eq. (10) from [40]. $d\Gamma/dq^2$ is normalized to the total rate in the $\ell = \mu$ case, Γ_μ , and the g_{V_L} and g_{V_R} curves overlap. For A_{FB} , the SM and g_{V_L} curves overlap, and for A_{λ_τ} , all three curves overlap.

left-handed and right-handed vector couplings given in [40], which we reproduce here in Eq. (10), and examine their impact on $R(J/\psi)$ and the angular observables for $B_c \rightarrow J/\psi$.

In Fig. 4 (left-hand plot), we see that the semitauonic differential rate increases very markedly for the best fit value of g_{V_L} or g_{V_R} inferred from $R(D^{(*)})$ [40]. This results in a corresponding 10σ increase of $R(J/\psi)$, to give the values below,

$$\begin{aligned} g_{V_R} &= -0.01 - i0.39; & R^{g_{V_R}}(J/\psi) &= 0.3022(44), \\ g_{V_L} &= 0.07 - i0.16; & R^{g_{V_L}}(J/\psi) &= 0.3022(44). \end{aligned} \quad (10)$$

The difference between $R(J/\psi)$ and $R^{g_{V_R/L}}(J/\psi)$ is then close to the difference between the SM and current experimental average value of $R(D^*)$ that g_{V_L} and g_{V_R} were designed to reproduce. Note, however, that our values for $R^{g_{V_R/L}}(J/\psi)$ are still in tension with the experimental result.

We also compute the angular observables defined in [40], which are relevant for $B_c^- \rightarrow J/\psi \ell^- \bar{\nu}_\ell$. These are the forward-backward asymmetry A_{FB} for the lepton ℓ (note that the forward direction is that of the J/ψ in Fig. 1), the lepton polarization asymmetry A_{λ_ℓ} , and the longitudinal polarization fraction for the J/ψ , $F_L^{J/\psi}$. Writing

$$\begin{aligned} \frac{d^2\Gamma}{dq^2 d\cos(\theta_W)} &= a_{\theta_W}(q^2) + b_{\theta_W}(q^2) \cos(\theta_W) \\ &\quad + c_{\theta_W}(q^2) \cos^2(\theta_W), \end{aligned} \quad (11)$$

the observables are defined as

$$\begin{aligned} A_{FB}(q^2) &= -\frac{b_{\theta_W}(q^2)}{d\Gamma/dq^2}, \\ A_{\lambda_\ell}(q^2) &= \frac{d\Gamma^{\lambda_\ell=-1/2}/dq^2 - d\Gamma^{\lambda_\ell=+1/2}/dq^2}{d\Gamma/dq^2}, \\ F_L^{J/\psi}(q^2) &= \frac{d\Gamma^{\lambda_{J/\psi}=0}/dq^2}{d\Gamma/dq^2}. \end{aligned} \quad (12)$$

A_{FB} and A_{λ_ℓ} are plotted as a function of q^2 in Fig. 4, showing both the behavior in the SM and the impact of the possible NP couplings g_{V_R} and g_{V_L} . Note the very different shape of the SM curves for A_{FB} and A_{λ_ℓ} in the SM compared to those for $\ell = e$ or μ given in [28]. The helicity -1 virtual W will throw a helicity $-1/2$ lepton predominantly in the W direction (i.e., backwards) but the mass of the τ changes the lepton helicity mixture. g_{V_R} accentuates this effect by boosting the contribution of $|H_+|^2$ but without changing the τ helicity mixture.

For an observable $O_i^\ell(q^2) = N_i^\ell(q^2)/D_i^\ell(q^2)$, the integrated quantities are defined as

$$\langle O_i^\ell \rangle = \int_{m_\ell^2}^{q_{\max}^2} N_i^\ell(q^2) dq^2 / \int_{m_\ell^2}^{q_{\max}^2} D_i^\ell(q^2) dq^2. \quad (13)$$

We give results for $\langle A_{\lambda_\tau} \rangle$, $\langle A_{FB} \rangle$, and $\langle F_L^{J/\psi} \rangle$ in Table III for $B_c^- \rightarrow J/\psi \tau^- \bar{\nu}_\tau$ in the SM and for the NP couplings g_{V_R} and

TABLE III. Integrated angular observables for $B_c^- \rightarrow J/\psi \tau^- \bar{\nu}_\tau$ in the SM and for possible NP left-handed and right-handed vector couplings from Eq. (10).

	SM	g_{V_R}	g_{V_L}
$\langle A_{FB} \rangle$	-0.058(12)	-0.0089(96)	-0.058(12)
$\langle A_{\lambda_\tau} \rangle$	0.5185(75)	0.5183(75)	0.5185(75)
$\langle F_L^{J/\psi} \rangle$	0.4416(92)	0.4423(92)	0.4416(92)

TABLE IV. LFUV variables for $B_c \rightarrow J/\psi$ defined in Eqs. (12), (13), and (14) [40]. The second column gives results in the SM and then the further two columns give results for NP couplings, in the τ channel only, of g_{V_R} and g_{V_L} [Eq. (10)].

	SM	g_{V_R}	g_{V_L}
$R(\mathcal{A}_{FB})$	0.255(38)	0.039(40)	0.255(38)
$R(\mathcal{A}_{\lambda_e})$	0.5216(74)	0.5214(74)	0.5216(74)
$R(F_L^{J/\psi})$	0.887(10)	0.889(10)	0.887(10)

g_{V_L} from Eq. (10). Our SM results agree within 2σ with those from a covariant light-front quark model that included information from our preliminary lattice QCD results [41].

We also construct the lepton flavor universality violating (LFUV) ratios,

$$R(O_i) = \frac{\langle O_i^\tau \rangle}{\frac{1}{2}(\langle O_i^\mu \rangle + \langle O_i^e \rangle)}. \quad (14)$$

These are given in Table IV, where we see that $R(\mathcal{A}_{FB})$ can distinguish between a NP right-handed vector coupling and a left-handed one. None of the other LFUV ratios change significantly from their SM values under the addition of either g_{V_R} or g_{V_L} . This is consistent with what was seen for $B \rightarrow D^* \ell \bar{\nu}_\ell$ in [40].

Conclusion.—We give the first computation in lattice QCD of the branching fraction ratio $R(J/\psi)$ that tests for lepton flavor universality in $B_c \rightarrow J/\psi$ semileptonic decay. Our value in the SM is $R(J/\psi) = 0.2582(38)$, with an error budget in Table II. This is in tension with the LHCb result at 1.8σ , where σ is the experimental uncertainty. The $B_c \rightarrow J/\psi$ form factors that we have calculated [28] to do this should enable the dominant systematic error in the experimental determination of $R(J/\psi)$ to be reduced, allowing progress towards an accurate test of the SM.

We illustrate how NP might show up in $B_c \rightarrow J/\psi$ decay with predictions for a variety of angular observables and τ to e/μ ratios both in the SM and with additional NP couplings consistent with the current average of experimental measurements of $B \rightarrow D^{(*)}$ decay. We have shown that $R(J/\psi)$ is close to the value of $R(D^*)$ both in the SM and in the presence of NP entering through either g_{V_R} or g_{V_L} . The resultant value of $R^{g_{V_R/L}}(J/\psi)$ is still in tension with the experimental value.

We are grateful to the MILC Collaboration for the use of their configurations and code. We thank C. Bouchard, B. Colquhoun, J. Koponen, P. Lepage, E. McLean, and C. McNeile for useful discussions. Computing was done on the Cambridge service for Data Driven Discovery (CSD3), part of which is operated by the University of Cambridge Research Computing on behalf of the DIRAC HPC Facility of the Science and Technology Facilities Council (STFC).

The DIRAC component of CSD3 was funded by BEIS capital funding via STFC capital Grants No. ST/P002307/1 and No. ST/R002452/1 and STFC operations Grant No. ST/R00689X/1. DiRAC is part of the national e-infrastructure. We are grateful to the CSD3 support staff for assistance. Funding for this work came from the UK Science and Technology Facilities Council Grants No. ST/L000466/1 and No. ST/P000746/1.

*judd.harrison@glasgow.ac.uk

†christine.davies@glasgow.ac.uk

‡http://www.physics.gla.ac.uk/HPQCD.

- [1] J. P. Lees *et al.* (BABAR Collaboration), Phys. Rev. Lett. **109**, 101802 (2012).
- [2] J. P. Lees *et al.* (BABAR Collaboration), Phys. Rev. D **88**, 072012 (2013).
- [3] M. Huschle *et al.* (Belle Collaboration), Phys. Rev. D **92**, 072014 (2015).
- [4] Y. Sato *et al.* (Belle Collaboration), Phys. Rev. D **94**, 072007 (2016).
- [5] S. Hirose *et al.* (Belle Collaboration), Phys. Rev. Lett. **118**, 211801 (2017).
- [6] S. Hirose *et al.* (Belle Collaboration), Phys. Rev. D **97**, 012004 (2018).
- [7] R. Aaij *et al.* (LHCb Collaboration), Phys. Rev. Lett. **115**, 111803 (2015); **115**, 159901(E) (2015).
- [8] R. Aaij *et al.* (LHCb Collaboration), Phys. Rev. Lett. **120**, 171802 (2018).
- [9] R. Aaij *et al.* (LHCb Collaboration), Phys. Rev. D **97**, 072013 (2018).
- [10] A. Abdesselam *et al.* (Belle Collaboration), arXiv: 1904.08794.
- [11] Y. Amhis *et al.* (HFLAV Collaboration), https://hflav.web.cern.ch (2019).
- [12] Y. S. Amhis *et al.* (HFLAV Collaboration), arXiv: 1909.12524.
- [13] F. U. Bernlochner, Z. Ligeti, M. Papucci, and D. J. Robinson, Phys. Rev. D **95**, 115008 (2017); **97**, 059902 (E) (2018).
- [14] D. Bigi, P. Gambino, and S. Schacht, J. High Energy Phys. **11** (2017) 061.
- [15] S. Jaiswal, S. Nandi, and S. K. Patra, J. High Energy Phys. **12** (2017) 060.
- [16] J. A. Bailey, A. Bazavov, C. Bernard, C. M. Bouchard, C. DeTar *et al.* (Fermilab Lattice and MILC Collaborations), Phys. Rev. D **89**, 114504 (2014).
- [17] J. Harrison, C. T. H. Davies, and M. Wingate (HPQCD Collaboration), Phys. Rev. D **97**, 054502 (2018).
- [18] A. Vaquero, C. DeTar, A. El-Khadra, A. Kronfeld, J. Laiho, and R. Van de Water, in *17th Conference on Flavor Physics and CP Violation* (2019) [arXiv:1906.01019].
- [19] A. Lytle, Proc. Sci. LATTICE2019 (2020) 228.
- [20] R. Aaij *et al.* (LHCb Collaboration), Phys. Rev. Lett. **120**, 121801 (2018).
- [21] A. Anisimov, I. Narodetsky, C. Semay, and B. Silvestre-Brac, Phys. Lett. B **452**, 129 (1999).
- [22] V. Kiselev, arXiv:hep-ph/0211021.

- [23] M. A. Ivanov, J. G. Korner, and P. Santorelli, *Phys. Rev. D* **73**, 054024 (2006).
- [24] E. Hernandez, J. Nieves, and J. M. Verde-Velasco, *Phys. Rev. D* **74**, 074008 (2006).
- [25] D. Leljak, B. Melic, and M. Patra, *J. High Energy Phys.* 05 (2019) 094.
- [26] A. Issadykov and M. A. Ivanov, *Phys. Lett. B* **783**, 178 (2018).
- [27] W. Wang and R. Zhu, *Int. J. Mod. Phys. A* **34**, 1950195 (2019).
- [28] J. Harrison, C. T. Davies, and A. Lytle (HPQCD Collaboration), companion paper, *Phys. Rev. D* **102**, 094518 (2020).
- [29] E. Follana, Q. Mason, C. Davies, K. Hornbostel, G. P. Lepage, J. Shigemitsu, H. Trottier, and K. Wong (HPQCD and UKQCD Collaborations), *Phys. Rev. D* **75**, 054502 (2007).
- [30] C. T. H. Davies, C. McNeile, E. Follana, G. P. Lepage, H. Na, and J. Shigemitsu, *Phys. Rev. D* **82**, 114504 (2010).
- [31] C. McNeile, C. T. H. Davies, E. Follana, K. Hornbostel, and G. P. Lepage (HPQCD Collaboration), *Phys. Rev. D* **85**, 031503(R) (2012).
- [32] C. McNeile, C. T. H. Davies, E. Follana, K. Hornbostel, and G. P. Lepage, *Phys. Rev. D* **86**, 074503 (2012).
- [33] A. Bazavov, C. Bernard, N. Brown, C. DeTar, A. X. El-Khadra *et al.*, *Phys. Rev. D* **98**, 074512 (2018).
- [34] E. McLean, C. T. H. Davies, A. T. Lytle, and J. Koponen, *Phys. Rev. D* **99**, 114512 (2019).
- [35] E. McLean, C. T. H. Davies, J. Koponen, and A. T. Lytle, *Phys. Rev. D* **101**, 074513 (2020).
- [36] T. D. Cohen, H. Lamm, and R. F. Lebed, *Phys. Rev. D* **98**, 034022 (2018).
- [37] A. Sirlin, *Nucl. Phys.* **B196**, 83 (1982).
- [38] J. D. Richman and P. R. Burchat, *Rev. Mod. Phys.* **67**, 893 (1995).
- [39] S. Bifani, S. Descotes-Genon, A. Romero Vidal, and M.-H. Schune, *J. Phys. G* **46**, 023001 (2019).
- [40] D. Bećirević, M. Fedele, I. Nišandžić, and A. Tayduganov, arXiv:1907.02257.
- [41] Z.-R. Huang, Y. Li, C.-D. Lu, M. A. Paracha, and C. Wang, *Phys. Rev. D* **98**, 095018 (2018).